

# Length scales coupling for nonlinear dynamical problems in magnetism

V. V. Dobrovitski,<sup>1</sup> M. I. Katsnelson,<sup>1,2</sup> and B. N. Harmon<sup>1</sup>

<sup>1</sup>*Ames Laboratory, Iowa State University, Ames, Iowa, 50011*

<sup>2</sup>*Institute of Metal Physics, Ekaterinburg 620219, Russia*

(Dated: October 31, 2018)

The dynamics of real magnets is often governed by several interacting processes taking place simultaneously at different length scales. For dynamical simulations the relevant length scales should be coupled, and the energy transfer accurately described. We show that in this case the micromagnetic theory is not always reliable. We present a coarse-graining approach applicable to nonlinear problems, which provides a unified description of all relevant length scales, allowing a smooth, seamless coupling. The simulations performed on model systems show that the coarse-graining approach achieves nearly the precision of all-atom simulations.

PACS numbers: 75.40.Mg, 75.60.Ej, 75.30.Hx, 02.70.Dh

The dynamics of magnetization in real magnets is often governed by defects: impurities, vacancies, grain boundaries, etc. They serve as nucleation centers for magnetization reversal or as pinning centers for domain walls (DW), due to very localized (several lattice constants) but significant changes in the magnetic interactions. As a result, the torques acting on individual atomic spins in the vicinity of the defect are strongly non-uniform at the atomic scale. These small-scale inhomogeneities can result, however, in large-scale (hundreds or thousands of angstroms) changes of the magnetization distribution (e.g. nucleation of a domain). At larger length scales (microns), the magnons propagate into the bulk of the sample carrying away significant energy. Such multiscale phenomena are encountered in the depinning of DW [1, 2, 3, 4], the influence of surfaces and interfaces on the spins in the bulk [5, 6, 7, 8], etc. These phenomena determine basic magnetic properties such as the coercive field and the dynamics of magnetization reversal.

Accurate simulations of such phenomena might be possible if all the interactions and dynamics could be treated at the atomic scale [9], but for a sample of the size of few tens of microns, the number of spins becomes much too large for modern supercomputers. Atomistic modeling can be used, however, for the regions close to the defects. For the large-scale processes occurring far from the defects a collective description should be used, e.g. micromagnetic (MM) theory. To simulate accurately the multiscale processes, all the relevant scales should be modeled simultaneously, and seamlessly coupled to describe correctly the energy transfer. The simplest solution would be to use the standard MM approach with gradually increasing resolution (reducing the size of the computational cell) near the defect, until every micromagnetic cell contains a single atomic spin. At this ultimate resolution, the micromagnetic Landau-Lifshitz-Gilbert equation coincides with the equation of precession of an individual atomic spin.

In this paper, using simulations performed on model 1-D chain systems, we show that such an approach is

often inadequate for length scale coupling, giving results which differ drastically from the exact solutions obtained by all-atom simulations. Thus, for an important class of dynamical problems in magnetism, a new approach is needed. Here, we present a theoretical framework along with a computational scheme, which allows treatment of all length scales in exactly the same manner, enabling a truly seamless linking of different scales. The proposed approach is applicable to essentially nonlinear problems, and yields reliable results which are in excellent agreement with exact atomic simulations.

Length scale coupling has been extensively discussed in the context of lattice dynamics modeling [10, 11, 12, 15] and successfully applied for the study of crack propagation and nanoindentation [13, 14, 16]. Analogous schemes can be constructed for linear magnetic problems [17], but most of the interesting problems in magnetism are essentially nonlinear due to the constraint  $S_x^2 + S_y^2 + S_z^2 = S^2$  ( $S_{x,y,z}$  are the components of the spin and  $S$  is its length; everywhere below we assume  $S = 1$ ). Moreover, the lattice constant  $a$  is the relevant length scale for a typical problem of lattice dynamics, while magnetic problems have one more intrinsic length scale, the DW width  $\Delta$ . Therefore, magnetic multiscale simulations present some unique problems.

Our approach to linking length scales in dynamical magnetic simulations is based on statistical coarse graining (CG), which has been successfully used before [12, 17] to define suitable collective variables (“gross variables”). For simplicity, we consider only the case of zero temperature, thus restricting the analysis to purely dynamical problems, with dissipation and thermal noise effects absent. We assume that the system under consideration is a ferromagnet made of identical classical spins  $\mathbf{S}_\mu$  ( $|\mathbf{S}_\mu| = 1$ ), located at the  $\mu$ -th site of the crystalline lattice (greek indices enumerate the atomic lattice sites). The system is described by a rather general spin Hamiltonian

$$\mathcal{H} = \mathcal{H}^0 + \mathcal{V}, \quad \mathcal{H}^0 = \sum_{\mu} \mathcal{H}_{\mu}^0 = \sum_{\mu, \nu} J_{\mu\nu} \mathbf{S}_{\mu} \mathbf{S}_{\nu}, \quad (1)$$

where  $\mathcal{H}^0$  describes the isotropic exchange interaction, while  $\mathcal{V} \ll \mathcal{H}^0$  represents all the other, much weaker interactions, and  $J_{\mu\nu}$  is the exchange interaction between the atomic spins at the sites  $\mu$  and  $\nu$ . We will need a Hamiltonian formulation of the magnetization dynamics, therefore below we describe spin by conjugate canonical variables  $\alpha_{1\mu} = 2 \sin(\theta_\mu/2) \cos \phi_\mu$  and  $\alpha_{2\mu} = 2 \sin(\theta_\mu/2) \sin \phi_\mu$ , where  $\theta_\mu$  and  $\phi_\mu$  are the azimuthal and the polar angles of the spin vector correspondingly. We assume that for the simulations of the large-scale regions located far from the defects, the finite-element method (FEM) is used. Thus, we define the gross variables, which describe the state of the system at a given length scale, by averaging the atomic degrees of freedom:  $\alpha_{1j} = \sum_\mu f_{\mu,j} \alpha_{1\mu}$ , and  $\alpha_{2j} = \sum_\mu f_{\mu,j} \alpha_{2\mu}$ , where the index  $j$  corresponds already to the computational FEM nodes. The weight function  $f_{\mu,j}$  localized near the node  $j$  must satisfy the normalization condition  $\sum_\mu f_{\mu,j} = 1$ . The choice of this function was discussed [17] for linear magnetic multiscale problems; our experience shows that the following piecewise-linear choice is sufficient:  $f_{\mu,j} = f_0 |\mu - \mu_j| / |\mu_j - \mu_{j-1}|$  for  $\mu \in [\mu_{j-1}, \mu_j]$ , where  $\mu_j$  is the atomic position of the  $j$ -th computational node and  $f_0$  is the normalization.

The main assumption of the approaches based on the coarse graining ideology (such as the non-equilibrium statistical operator [18] or projection operator [19] methods) is that the atomic degrees of freedom are in local equilibrium, and the equilibrium conditions are determined by the gross variables [20]. This means that all atomic spins located near the node  $j$  are nearly parallel to the direction defined by the the variables  $\alpha_{1,2j}$ ; the exchange part  $\mathcal{H}_0$  of the Hamiltonian (1) is responsible for that (thus, the coarse-graining approach can be used also for finite temperature if it is small in comparison with the Curie temperature). Then, the distribution function for the atomic variables is

$$\begin{aligned} \rho &= Q^{-1} \exp(-\beta \mathcal{H}'), \\ \mathcal{H}' &= \mathcal{H}^0 + \sum_{\mu,j} F_j f_{\mu,j} \alpha_{1\mu} + \sum_{\mu,j} G_j f_{\mu,j} \alpha_{2\mu}, \end{aligned} \quad (2)$$

where  $Q$  is the statistical integral, and the torques  $F_j$  and  $G_j$  are determined from the conditions of local equilibrium:  $\sum_\mu f_{\mu,j} \langle \alpha_{1\mu} \rangle = \alpha_{1j}$ , and  $\sum_\mu f_{\mu,j} \langle \alpha_{2\mu} \rangle = \alpha_{2j}$ , where the angular brackets mean the statistical averaging with the distribution function (2).

However, the exchange Hamiltonian  $\mathcal{H}_0$  is rotationally invariant, and a zero-frequency mode is present in the statistical integral  $Q$  in Eq. 2. In the linear approximation, this leads to a divergence, and the account of nonlinear effects becomes possible. Such a situation has been studied e.g. by Bogoliubov in the work on the small polaron problem, see e.g. Ref. [21]. The general ideas of that work can be applied here.

We need to separate the (nonlinear) motion of gross

variables from the (quasilinear) motion of the atomic-scale variables to exclude the secular terms causing divergence of  $Q$ . To do this, we note that the characteristic scale of nonlinear magnetic structures, the DW width  $\Delta$ , is much bigger than the interatomic distance  $a$ , and the separation of the slow and the fast variables can be done in the spirit of the modified adiabatic theory [21]. Instead of using the parameters  $\alpha_{1,2j}$ , we define a local coordinate frame, rotated with respect to the "laboratory" frame by the angles  $\theta_j$  and  $\phi_j$  such that  $\alpha_{1j} = 2 \sin(\theta_j/2) \cos \phi_j$  and  $\alpha_{2j} = 2 \sin(\theta_j/2) \sin \phi_j$ . To exclude the secular terms, we use the condition  $\sum_\mu f_{\mu,j} \langle \alpha_{1\mu}^{(j)} \rangle = \sum_\mu f_{\mu,j} \langle \alpha_{2\mu}^{(j)} \rangle = 0$ , where  $\alpha_{1,2\mu}^{(j)}$  are defined already in the local coordinate frame associated with  $j$ -th node. These conditions are local, since the weighting function  $f_{\mu,j}$  is local, and the statistical integral  $Q$  is also calculated in the local coordinate frame. As a result, the equations of motion for the gross variables  $\theta_j$  and  $\phi_j$  can be obtained in closed form:

$$\begin{aligned} \dot{\theta}_j &= - \sum_\mu f_{\mu,j} \langle \partial \mathcal{V} / \partial \alpha_{2,\mu} \rangle + \sum_{kn} M_{jk} D_{kn} \alpha_{2n}^{(j)}, \\ \sin \theta_j \dot{\phi}_j &= \sum_\mu f_{\mu,j} \langle \partial \mathcal{V} / \partial \alpha_{1,\mu} \rangle - \sum_{kn} M_{jk} D_{kn} \alpha_{1n}^{(j)}, \end{aligned} \quad (3)$$

where  $M_{jk} = \sum_\mu f_{\mu,j} f_{\mu,k}$ , and  $D_{jk} = D_{jk}^0 - d_j S_k / S_0 - d_k S_j / S_0 + d_0 S_j S_k / S_0^2$ , where  $D_{jk}^0 = \left( \sum_{\mu\nu} f_{\mu,j} \mathcal{J}_{\mu\nu}^{-1} f_{\nu,k} \right)^{-1}$ ,  $\mathcal{J}_{\mu\nu}$  is the Hessian matrix of the exchange Hamiltonian,  $S_k$  is the eigenvector of  $D_{jk}^0$  corresponding to the zero eigenvalue, and  $d_j = \sum_l D_{jl}^0$ ,  $d_0 = \sum_l d_l$ ,  $S_0 = \sum_l S_l$ . Note that the matrices  $M$  and  $D$  should be calculated only once and used later during simulations.

Now, let us focus on the numerical results obtained using the procedure described above. The first case tests the ability of our CG scheme to handle the dynamics of an essentially nonlinear object, e.g. a domain wall. We consider a 1-D chain of  $N = 465$  spins with ferromagnetic nearest-neighbor coupling  $J = 25$ , and antiferromagnetic next-nearest-neighbor coupling  $J' = -\gamma J = -2.5$ . The spins possess single-ion anisotropy of easy-axis type,  $K = 0.01$  (the easy axis is directed along the  $y$ -direction); the dipole-dipole interactions are neglected for simplicity. The ends of the chain are different from the bulk; this represents e.g. a nanowire which has the growth defects at the ends causing the spin Hamiltonian parameters  $J$ ,  $J'$  and  $K$  to be different from their bulk values. Thus, six spins at one end of the chain are chosen to have the following parameters:  $J_{01} = 0.5J$ ,  $J_{12} = 0.6J$ ,  $J_{23} = 0.7J$ ,  $J_{34} = 0.8J$ ,  $J_{45} = J$ ,  $J_{56} = J$ ,  $K_0 = -0.4K$ ,  $K_1 = -0.2K$ ,  $K_2 = 0$ ,  $K_3 = 0.2K$ ,  $K_4 = 0.4K$ ,  $K_5 = 0.8K$ . At the other end of the chain, the last six spins have the same parameters in reverse order. Initially, the chain contains a Neel DW, with spins rotating in the  $x$ - $y$  plane from the direction along the  $y$ -axis to the opposite direction.

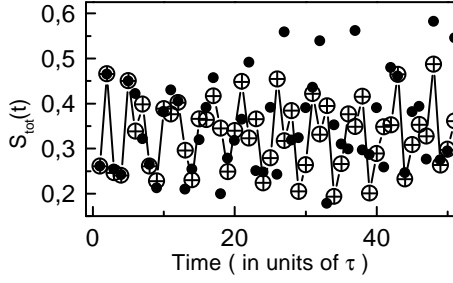


FIG. 1: Time dependence of the total magnetization  $S_{\text{tot}}(t)$  of the chain calculated by three methods: large white circles — atomic simulations, small black circles — MM simulations, crosses — CG scheme. Initial conditions correspond to the Neel domain wall. Since the CG results almost coincide with the atomistic ones, the crosses appear mostly in the centers of the white circles.

At  $t = 0$ , the external field  $H = 0.01$  is applied in the  $x$ - $y$  plane, at the angle  $\phi = -0.4\pi$  with the  $x$ -axis. As a result, the wall starts moving. After hitting one end of the chain, it deforms, and reflects, moving to the other end of the chain. Note that, since we omit dissipation and fluctuations, the energy of the system is conserved, and the dynamics of the system is quasi-periodic.

To compare the performance of different computational schemes, we have modeled the system's dynamics by (1) atomic simulations which give the exact solution, (2) by micromagnetic simulations using the method suggested in Ref. [22], with the number of spins in the cell varying from five (in the middle of the chain) to one (at the ends), and (3) by the CG scheme described above, with the same grid as used in the MM simulations. The computational time step, along with all other relevant parameters, has been kept the same for all schemes. The temporal dependence of the chain's total magnetization  $S_{\text{tot}}(t) = \sqrt{S_x^2(t) + S_y^2(t) + S_z^2(t)}$  is shown in Fig. 1, where the time is measured in units of  $\tau = 0.4\pi/|H \sin \phi| \approx 132$ . As one can see, the MM simulations (black circles) differ considerably from the exact atomistic solution, while the CG scheme gives results practically coinciding with the atomistic simulations. The same conclusion can be drawn from Fig. 2, where the magnetization profile in the chain is shown at  $t = 60\tau$ ; the magnetization direction at every atomic site  $\mathbf{S}_\mu$  is characterized by the two angles,  $\omega_\mu$  and  $\psi_\mu$  such that  $S_\mu^x = \sin \omega_\mu \cos \psi_\mu$ ,  $S_\mu^y = \cos \omega_\mu$  (since the easy axis coincides with the  $y$ -axis), and  $S_\mu^z = \sin \omega_\mu \sin \psi_\mu$ .

A similar set of simulations has also been performed to study the magnetization reversal in the chain. The system, along with all simulation parameters, has been kept the same as described above, but the initial condition represents a chain magnetized to saturation,  $S_\mu^y = 1$  for all  $\mu$ . At  $t = 0$ , again, the external field  $H = 0.02$  has been applied, at the angle  $\phi = -0.4\pi$  to the  $x$ -axis.

Since we are studying an energy-conserving case, in

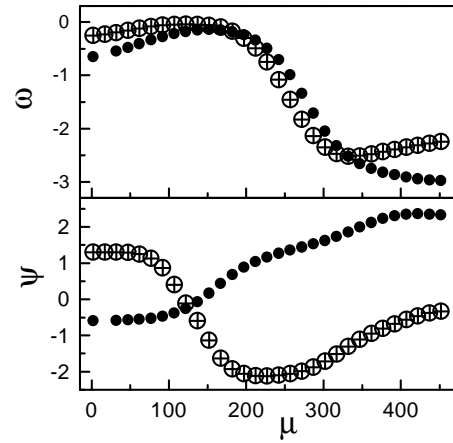


FIG. 2: The magnetization profile in the chain (the angles  $\omega_\mu$  and  $\psi_\mu$ ) at  $t = 60\tau$  calculated by three methods: large white circles — atomic simulations, small black circles — MM sim-

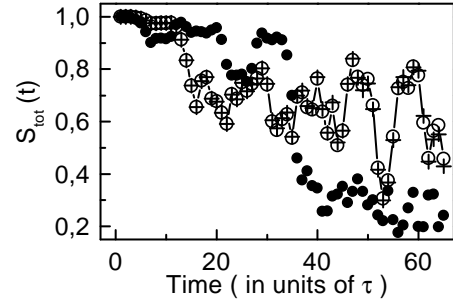


FIG. 3: Time dependence of the total magnetization  $S_{\text{tot}}(t)$  of the chain calculated by three methods: large white circles — atomic simulations, small black circles — MM simulations, crosses — CG scheme. Initial conditions correspond to chain uniformly magnetized along the  $y$ -axis. Since the CG results almost coincide with the atomistic ones, the crosses appear mostly in the centers of the white circles.

the absence of the defects at the ends of the chain, all the spins would rotate in unison. However, in the presence of the perturbation caused by the defects, different spins rotate with slightly different rates, and the system's motion becomes stochastic. Therefore, after some time, the Zeeman energy is transferred to the energy of short-wavelength magnons, leading to a gradual decrease of the system's total magnetization [23, 24].

The chain's total magnetization as functions of time is shown in Fig. 3, with the time unit  $\tau = 0.4\pi/|H \sin \phi| \approx 66$ . Magnetization profiles at  $t = 60\tau$  are presented in Fig. 4. Again, one can see that the MM approach does not describe the behavior of the system correctly even at a qualitative level. The CG scheme performs much

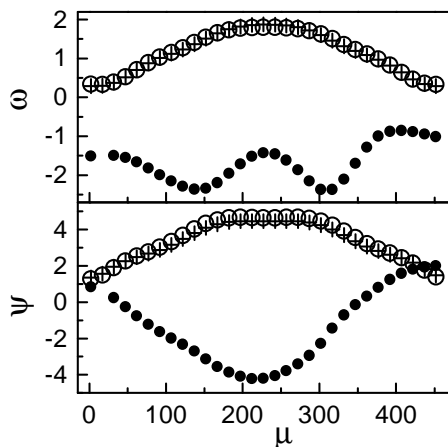


FIG. 4: The magnetization profile in the chain (the angles  $\omega_\mu$  and  $\psi_\mu$ ) at  $t = 60\tau$  calculated by three methods: large white circles — atomic simulations, small black circles — MM simulations, crosses — CG scheme. Initial conditions correspond to chain uniformly magnetized along the  $y$ -axis.

better, giving the results very close to the exact atomistic solution.

Such a drastic difference in the two schemes, CG and MM, is caused by the essential nonlinearity of magnetization dynamics. Due to the presence of atomic-scale inhomogeneities, in the course of the system's motion, a considerable number of short-wavelength excitations are generated near the defect. Wavelengths of these magnons are smaller than the size of the computational cell, and the micromagnetic theory neglects them completely, although the collective effect of a large number of such modes is significant. In contrast, the coarse-graining approach does take the atomic-scale modes into account, and describes very well the collective properties of an ensemble of these short-wavelength excitations.

In summary, we have shown that the standard micromagnetic theory does not handle correctly the dynamics of nonlinear multiscale magnetic processes. We have suggested another approach, based on statistical coarse graining, which is applicable to nonlinear problems. Numerical tests on 1-D systems show that the CG scheme, in contrast with the MM approach, gives almost exact results for rather large time spans. It is worthwhile to note that the only essential ingredient of the coarse graining approach is the standard theory of local equilibrium. Therefore, the CG scheme can be applied to a large set of 2-D and 3-D problems, including dissipation, thermal noise, interaction with other degrees of freedom (spin-phonon interactions) etc.

The authors would like to thank J. Morris, R. Sabiryanov, and R. Rudd for helpful discussions. This work was partially carried out at the Ames Laboratory, which is operated for the U. S. Department of Energy by

Iowa State University under Contract No. W-7405-82 and was supported by the Director of the Office of Science, Office of Basic Energy Research of the U. S. Department of Energy. This work was partially supported by Russian Foundation for Basic Research, grant 00-02-16086.

- 
- [1] L. Lopez-Diaz, E. Della Torre, and E. Moro, *J. Appl. Phys.* **85**, 4367 (1999).
  - [2] T. G. Pokhil, *J. Appl. Phys.* **81**, 5035 (1997).
  - [3] A. Melsheimer and H. Kronmüller, *Physica B: Cond. Matter*, **299**, 251 (2001).
  - [4] S.-s. Yan, R. Schreiber, P. Grünberg, and R. Schäfer, *J. Magn. Magn. Mater.* **210**, 309 (2000).
  - [5] R. H. Kodama, S. A. Makhlof, and A. E. Berkowitz, *Phys. Rev. Lett.* **79**, 1393 (1997).
  - [6] M. Jamet, W. Wernsdorfer, C. Thirion, et al., *Phys. Rev. Lett.* **86**, 4676 (2001).
  - [7] X. Amils, J. Nogués, S. Suriñach, et al., *Phys. Rev. B* **63**, 052402 (2001).
  - [8] J. G. Deak, R. H. Koch, *J. Magn. Magn. Mater.* **213**, 25 (2000).
  - [9] D. P. Landau, A. Bunker, and K. Chen, *Int. J. Mod. Phys. C* **7**, 401 (1996).
  - [10] S. Kohlhoff, P. Gumbach, and H. F. Fischmeister, *Phil. Mag. A* **64**, 851 (1991).
  - [11] E. B. Tadmor, M. Ortiz, and R. Philips, *Phil. Mag. A* **73**, 1529 (1996).
  - [12] R. E. Rudd and J. Q. Broughton, *Phys. Rev. B* **58**, R 5893 (1998).
  - [13] R. E. Rudd and J. Q. Broughton, *phys. stat. sol. (b)* **217**, 251 (2000).
  - [14] G. S. Smith, E. B. Tadmor, and Efthimios Kaxiras, *Phys. Rev. Lett.* **84**, 1260 (2000).
  - [15] W. Cai, M. de Koning, V. V. Bulatov and S. Yip, *Phys. Rev. Lett.* **85**, 3213 (2000).
  - [16] E. Lidorikis, M. E. Bachlechner, R. K. Kalia, et al., *Phys. Rev. Lett.* **87**, 086104 (2001).
  - [17] V. V. Dobrovitski, M. I. Katsnelson, B. N. Harmon, *J. Magn. Magn. Mater.* **221**, L235 (2000).
  - [18] D. N. Zubarev, *Nonequilibrium Statistical Thermodynamics* (Consultants Bureau, New York, 1974).
  - [19] H. Mori, *Progr. Theor. Phys.* **34**, 399 (1965).
  - [20] Similar ideas have been used to simulate the linear regime of the large-scale modes in the MM theory, see e.g. A. Lyberatos and R. W. Chantrell, *J. Phys. D: Appl. Phys.* **29**, 2332 (1996); M. A. Wongsam, J. D. Hannay, G. W. Roberts, and R. W. Chantrell, *J. Magn. Magn. Mater.* **200**, 649 (1999).
  - [21] N. N. Bogoliubov, and N. N. Bogoliubov, Jr., *Polaron theory: model problems* (Gordon and Breach, Amsterdam, 2000), Chapter 2.3.
  - [22] W. Chen, D. R. Fredkin, and T. R. Koehler, *IEEE Trans. Magn.* **29**, 2124 (1993).
  - [23] V. Safonov and H. N. Bertram, *J. Appl. Phys.* **85**, 5072 (1999).
  - [24] E. D. Boerner, H. N. Bertram, and H. Suhl, *J. Appl. Phys.* **87**, 5389 (2000).